AMPA receptor activation and phosphatase inhibition affect neonatal rat respiratory rhythm generation

Qing Ge* and Jack L. Feldman*†

*Departments of *Physiological Science and †Neurobiology, University of California, Los Angeles, CA 90095-1763, USA*

(Received 1 September 1997; accepted after revision 26 January 1998)

1. We investigated the role of α-amino-3-hydroxy-5-methylisoxazole-4-propionate (AMPA) receptors and their regulation in affecting respiratory-related neurones in a neonatal rat medullary slice that spontaneously generates respiratory-related rhythm and motor output in the hypoglossal (XII) nerve.

2. Bath application of the AMPA receptor antagonist 1-(4-aminophenyl)-4-methyl-7,8-methylenedioxy-5H-2,3-benzodiazepine (GYKI) completely blocked XII nerve activity, as well as respiratory-related synaptic drives in neurones within the preBötzinger Complex (preBötC), site of rhythm generation in the slice.

3. Local application of GYKI to the preBötC blocked respiratory rhythm. Local application of AMPA to the preBötC increased rhythm frequency and depolarized respiratory-related neurones.

4. In the presence of tetrodotoxin (TTX), GYKI completely blocked the inward current induced by local application of AMPA, but not that induced by kainate.

5. Local application of okadaic acid, a membrane-permeable inhibitor of phosphatase 1 and 2A, to the preBötC increased the frequency of respiratory motor discharge.

6. Intracellular application of microcystin, a membrane-impermeable inhibitor of phosphatase 1 and 2A, enhanced endogenous inspiratory drive and exogenous AMPA-induced current (in the presence of TTX) in preBötC inspiratory neurones. Both the enhanced inspiratory drive and the increased AMPA-induced current were completely blocked by GYKI.

7. We suggest that AMPA receptor activation and AMPA receptor modulation by phosphorylation are crucial for the rhythm generation within the preBötC.

Glutamate receptors mediate a major component of excitatory synaptic transmission in the central nervous system of mammals. For the rhythm generation of breathing and subsequent transmission of respiratory drive to motoneurones, the activation of non-*N*-methyl-D-aspartate (non-NMDA) glutamate receptors is necessary in neonatal mammals *in vitro* (Greer, Smith & Feldman, 1991; Smith, Ellenberger, Ballanyi, Richter & Feldman, 1991; Funk, Smith & Feldman, 1993). In a slice of rodent medulla that spontaneously generates respiratory-related rhythm and motor output in the hypoglossal (XII) nerve, glutamate stimulates, and non-NMDA receptor antagonists block, respiratory activity (Smith *et al.* 1991; Funk *et al.* 1993). While exogenous application of NMDA increases respiratory outflow, NMDA antagonists have little effect in neonates *in vitro* (Greer *et al.* 1991; Funk *et al.* 1993); they do, however, affect adult rats and cats (Connelly, Otto-Smith & Feldman, 1992; Pierrefiche, Foutz, Champagnat & Denavit-Saubié, 1994). That neonatal NMDAR1 knockout mice breathe *in vivo* and have virtually normal respiratory patterns *in vitro* further rules out an obligatory role for NMDA receptors in neonatal respiratory rhythm generation or drive transmission (Funk, Johnson, Smith, Dong, Lai & Feldman, 1997). In addition, cyclothiazide, which blocks AMPA receptor desensitization, but may also affect presynaptic release (Diamond & Jahr, 1995) or other AMPA receptor properties (Trussell, Zhang & Raman, 1993), increases the amplitude and frequency of respiratory motor output (Funk, Smith & Feldman, 1995), suggesting the involvement of AMPA receptors in respiratory pattern formation.

In this study, we examined specifically the role of AMPA receptors in the functional rhythm-generating network within the preBötzinger Complex (preBötC; Smith *et al.* 1991). We studied endogenous AMPA receptor activation in respiratory neurones using GYKI, a non-competitive AMPA

receptor antagonist (Donevan & Rogawski, 1993; Zorumski, Yamada, Price & Olney, 1993; Paternain, Morales & Lerma, 1995; Wilding & Huettner, 1995). By acting on an allosteric modulatory site on AMPA receptors (Ito, Tanabe, Kohda & Sugiyama, 1990; Donevan & Rogawski, 1993; Zorumski *et al.* 1993), which is absent in kainate receptors (Lerma, Paternain, Naranjo & Mellström, 1993; Patneau, Wright, Winters, Mayer & Gallo, 1994), GYKI completely blocks AMPA receptor-mediated currents but minimally affects kainate-induced responses at kainate receptors (Paternain *et al.* 1995).

In many regions of the mammalian brain, AMPA receptor function is affected by phosphorylation of its subunits or associated proteins (McGlade-McCulloh, Yamamoto, Tan, Brickey & Soderling, 1993; Blackstone, Murphy, Moss, Baraban & Huganir, 1994; Tan, Wenthold & Soderling, 1994; Nakazawa, Mikawa, Hashikawa & Ito, 1995; Yakel, Vissavajjhala, Derkach, Brickey & Soderling, 1995; Roche, O'Brien, Mammen, Bernhardt & Huganir, 1996; Barria, Muller, Derkach, Griffith & Soderling, 1997), which modulates synaptic activity (Greengard, Jen, Nairn & Stevens, 1991; McGlade-McCulloh *et al.* 1993; Blackstone *et al.* 1994; Wang, Dudek, Browning & MacDonald, 1994*a*; Roche *et al.* 1996). Since our preliminary observations indicated a critical role of AMPA receptors in rhythm generation in the slice, we hypothesized that phosphorylation of these receptors and/or associated proteins is an important mechanism for modulating respiratory pattern. As an initial test of this hypothesis, we examined the effect of local application of okadaic acid, a membrane-permeable phosphatase inhibitor, to the preBötC on respiratory rhythm. We then determined the effect on neuronal excitability by introducing microcystin, a membrane-impermeable phosphatase inhibitor, into preBötC respiratory neurones.

METHODS

Slice preparation

Experiments were performed on a medullary slice preparation spontaneously generating respiratory pattern (Smith *et al.* 1991). Briefly, Sprague–Dawley neonatal rats (age, 0–3 days) were anaesthetized with ether, decerebrated, and the neuraxis was isolated. The *en bloc* brainstem–spinal cord was pinned down with the ventral surface facing upwards and mounted in the specimen vice of a Vibratome (VT 1000, Technical Products International, St Louis, MO, USA) oriented vertically (rostral end upwards). It was then sectioned serially in the transverse plane until the landmarks at the rostral boundary of the preBötC, i.e. nucleus ambiguus and inferior olive, were visible. One transverse slice (600–750 μm thick) containing the preBötC was cut. The slice was transferred to a recording chamber (8–10 ml volume), and pinned down on a Sylgard elastomer. In experiments where rapid bath application of drug was desirable (e.g. fast blocking of synaptic transmission by TTX), a 0·9 ml recording chamber was used instead. The standard bath solution for dissection and slicing contained (mM): 128 NaCl, 3·0 KCl, 1·5 $CaCl_2$, 1·0 $MgSO_4$, 23·5 $NaHCO_3$, 0·5 NaH_2PO_4, 30 glucose and 1 ascorbic acid, bubbled with 95% O_2–5% CO_2 at room temperature (22–24 °C). During electrophysiological recording, the slice was continuously superfused (10–20 ml min^{-1}) with the standard solution with increased KCl (9 mM), and was recycled into a 200 ml reservoir equilibrated with 95% O_2–5% CO_2 at 27 ± 0·5 °C. Nerve activity was recorded from the cut end of the XII nerve with a suction electrode.

Whole-cell recordings from preBötC respiratory neurones

Blind whole-cell patch-clamp recordings were made from respiratory neurones in the preBötC (Smith *et al.* 1991). Patch electrodes were pulled from borosilicate glass (Model P-87, Sutter Instruments) with a tip size of 1–1·5 μm (4–6·5 MΩ). Electrodes were filled with a solution containing (mM): 120 potassium gluconate, 5·0 NaCl, 1·0 $CaCl_2$, 10 BAPTA (tetra-K^+ salt) and 2·0 ATP (Mg^{2+} salt); pH adjusted to 7·3 using KOH. Intracellular signals were amplified (Axopatch-1D, Axon Instruments). Electrodes were mounted on a microdrive and positioned over the preBötC. Positive pressure (150–180 mmHg) was applied to the electrodes as they were advanced 100 μm below the surface of the slice. The positive pressure was then released and the electrode advanced in 1 μm steps until a rapid increase in electrode resistance was observed. A slight negative pressure was applied to form a gigaohm (> 1 GΩ) seal. Cells were then ruptured using short-duration negative pressure pulses. Whole-cell capacitance was compensated and series resistance was compensated 60–90%. Cells with large, unstable access resistance (> 40 MΩ), indicating inadequate membrane rupture, were not used. The junction potential between bath solution and pipette filling solution was corrected in the values reported in this study.

Drug application

In experiments where GYKI was bath applied, one neurone was studied per slice because incomplete washout of GYKI prevented re-establishment of control conditions. In local application experiments, single- or multi-barrel pressure ejection pipettes (tip diameter, 6–8 μm per barrel: pressure, 50–70 kPa) were positioned over or beneath the rostral surface of the preBötC. GYKI or okadaic acid was microinjected into the tissue, while AMPA or kainate was perfused over the slice to avoid perturbing whole-cell recording in the same area. Injection volumes were determined by measuring the displacement of the pipette fluid meniscus with a microscope equipped with a calibrated eyepiece reticule. In perfusion experiments, the tip of the application pipette was first painted with ink to make it clearly visible when advancing towards the slice. After gently touching the slice surface under visual inspection, the pipette was quickly withdrawn by about 50 μm so that the ejection would be close to the surface while minimizing pressure artefacts. Slices were oriented so that the direction of superfusate flowed from dorsal to ventral to minimize spread of drugs to the XII motor nucleus or other neuronal populations dorsal to the preBötC. The buffer solution for each drug was applied as control. In experiments where the change in AMPA-induced current was monitored, only neurones within 160 μm of the slice surface were used, in order to ensure effective and consistent perfusion. All agonist-induced currents were allowed to return to the steady state for at least 15 s before another local application.

Microcystin was applied intracellularly via dialysis from the patch-clamp recording pipette solution. Microcystin stock solution was dissolved in DMSO or ethanol. Okadaic acid stock solution was prepared using minimal DMSO. The concentration of DMSO (v/v) in okadaic acid (OA) solutions was: 100 μM OA, 1·6%; 30 μM OA, 0·48%; 10 μM OA, 0·16%; 250 nM OA, 0·004%. GYKI (GYKI 52466), microcystin-LR, AMPA-HBr and kainate were obtained from RBI. Okadaic acid was obtained from Calbiochem. All

other drugs, including TTX and components of the recording pipette solution, bath and buffer solution were obtained from Sigma.

Data analysis

Signals were recorded on tape. Selected segments of whole-cell recording data were filtered and digitized at 1–2 kHz per channel and analysed using Axoscope software (Axon Instruments). To quantify the change in inspiratory drive or AMPA-induced current due to phosphatase inhibition, currents were integrated using pCLAMP software (Axon Instruments). Zero baseline for integration was set at the steady-state membrane current. For each neurone, the duration of integration was set to enclose the longest inspiratory drive or AMPA-induced current. This duration was then fixed for integration of all the inspiratory drives or AMPA-induced currents for this neurone. Periods of the respiratory rhythm at the XII nerve were obtained using AxoData and AxoGraph software (Axon Instruments).

The concentration-dependent effect of okadaic acid on respiratory rhythm period was analysed using non-linear regression. The average normalized ratio of maximal enhancement in inspiratory drive charge transfer and AMPA-induced charge transfer for inspiratory neurones with microcystin were analysed using Student's unpaired t test.

RESULTS

GYKI blocks endogenous inspiratory drive and exogenous AMPA-induced current

To determine the effect of endogenous AMPA receptor activation on respiratory motor pattern, GYKI was bath applied, where it could affect glutamate transmission among respiratory rhythm-generating neurones, premotoneurones and motoneurones. GYKI ($\geqslant 50\ \mu$M; $n = 7$) completely blocked XII nerve discharge, as well as the rhythmic activity of both inspiratory (I) and expiratory (E) neurones (Fig. 1*A* and *B*). Spontaneous excitatory postsynaptic potentials (sEPSPs) in these neurones were also blocked. Complete blockade took ~12–15 min with 50 μM GYKI ($n = 4$). Higher concentrations of GYKI (e.g. 100 μM; $n = 3$) shortened the blocking time to ~10 min. After 35–40 min washout time, the rhythm in both XII nerve and respiratory neurones partially recovered ($n = 3$; data not shown). In some slices, GYKI decreased respiratory frequency before it decreased the amplitude of the integrated XII nerve discharge; in others, the effect was reversed.

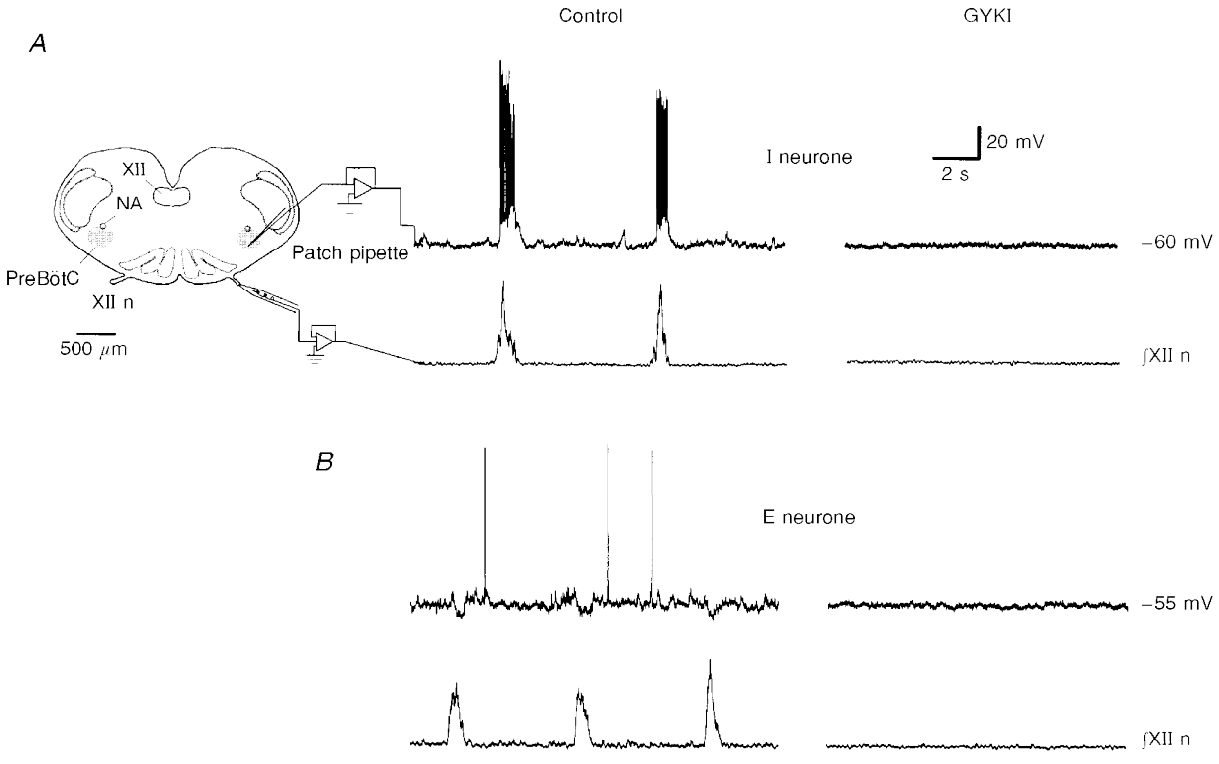

Figure 1. Bath application of GYKI blocked respiratory motor output and rhythmic activity of respiratory neurones

A, medullary slice preparation spontaneously generates respiratory-related pattern in the XII nerve. Inspiratory drive and sEPSPs of a typical preBötC inspiratory (I) neurone (holding current, $I_h = -56$ pA; membrane potential, $V_m = -60$ mV) were completely blocked 12 min after GYKI (50 μM) application (top trace). NA, nucleus ambiguus. XII, hypoglossal nucleus. XII n, hypoglossal nerve. *B*, inspiratory-modulated IPSPs and sEPSPs in a representative expiratory (E) neurone ($I_h = -66$ pA; $V_m = -55$ mV) were completely blocked 14 min after GYKI (50 μM) application (top trace). In both *A* and *B*, respiratory motor discharge in the XII nerve was completely blocked by GYKI (∫XII n).

GYKI (2·0 mM, $n = 3$; or 3·8 mM, $n = 2$), when microinjected within the preBötC, either ipsilateral or contralateral to the recorded XII nerve, reversibly blocked XII nerve discharge (Fig. 2). Control injections with GYKI buffer solution had no blocking effect on the motor output ($n = 3$; data not shown).

When we locally perfused AMPA (100 μM, 1 or 2 s) over the rostral surface of the preBötC, both inspiratory (Fig. 3*A*, top) and expiratory (Fig. 3*A*, middle) neurones ($n = 11$) depolarized (12–25 mV), and the respiratory frequency in the XII nerve increased by 44–217% (Fig. 3*A*, bottom; $n = 11$). Local application of kainate to the preBötC also depolarized respiratory neurones (data not shown). In order to identify the effects of GYKI on AMPA- or kainate-induced currents, TTX (0·5 μM) was bath applied. Subsequently, AMPA (100 μM) or kainate (1·0 mM) was locally applied to the preBötC, before and after bath application of GYKI (100 μM, 12–15 min). Both AMPA and kainate caused inward currents in respiratory neurones (Fig. 3*B*; $n = 25$ for AMPA, $n = 4$ for kainate). GYKI completely blocked the AMPA-induced currents (Fig. 3*B*, top; $n = 5$); while it only partially reduced the kainate-induced currents (Fig. 3*B*, bottom; $n = 3$).

Phosphatase inhibition within the preBötC increased the frequency of respiratory rhythm

To determine the effect of phosphatase inhibition on the rhythm generation network, we locally applied okadaic acid to the preBötC. In some experiments ($n = 3$), (+)-5-methyl-10,11-dihydro-5H-dibenzo[a,d]cyclohepten-5,10-imin maleate (MK-801; 100 μM) was added to the bath before application of okadaic acid to control for the possible effect of activation of NMDA receptors; since the effect of okadaic acid was comparable with or without MK-801, we pooled the data (Fig. 4). Okadaic acid induced a concentration-dependent increase in frequency of the XII nerve activity (Fig. 4*E*).

Phosphatase inhibition enhanced endogenous inspiratory drive and exogenous AMPA-induced current in inspiratory neurones

To determine the effect of phosphatase inhibition on respiratory neurones, microcystin was applied intracellularly.

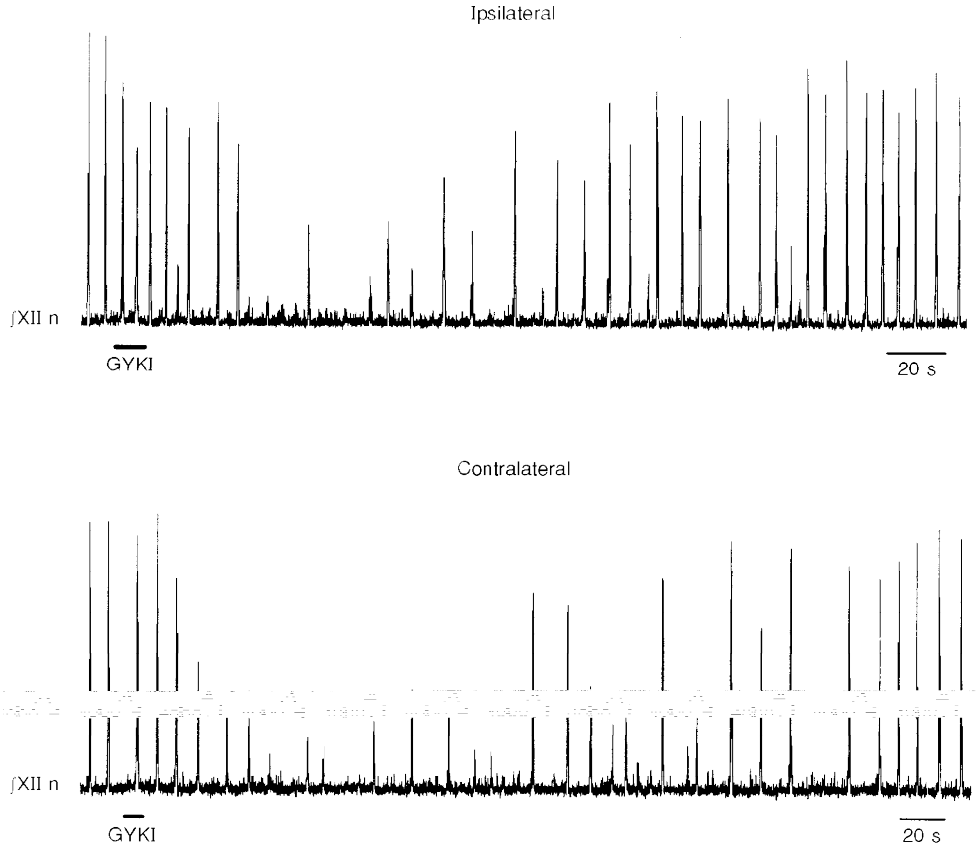

Figure 2. Local application of GYKI in the preBötC reversibly blocked XII nerve motor discharge

Unilateral local microinjection of GYKI (3·8 mM) within the preBötC reversibly blocked ipsilateral (top) and contralateral (bottom) XII nerve motor output. Longer injections (e.g. 20 s, 2·0 mM GYKI) completely blocked the XII nerve activity (data not shown).

Microcystin (50 μM) increased the duration, amplitude, or both, of inspiratory drive in inspiratory neurones ($n = 10$); the amplitude of sEPSPs/sEPSCs also increased (Fig. 5). Lower concentrations of microcystin were less effective (data not shown). The microcystin-enhanced inspiratory drive potential or current, and sEPSPs were completely blocked by bath application of GYKI (50 μM, Fig. 5). Because the time course of inspiratory drive current varied amongst inspiratory neurones, and the extent of change in amplitude or duration due to microcystin varied, the integral (instead of peak or decay time constant) of the drive current, i.e. charge transfer, was used as an index for this enhancement. Microcystin enhanced the endogenous inspiratory drive ($P < 0{\cdot}05$, Student's t test). The ratio of maximal enhancement in charge transfer (with respect to the state at the beginning of each recording), when averaged amongst inspiratory neurones dialysed with microcystin ($V_h = -60$ mV; $n = 5$; $175 \pm 14\%$, mean $\pm$ S.E.M.), was significant in comparison with the control inspiratory neurones ($V_h = -60$ mV; $n = 4$; $69 \pm 25\%$) (Fig. 5*E*). The enhancement in inspiratory drive due to microcystin was transient, with a maximum increase that occurred from 8 to 30 min after whole-cell break-in. Recordings from different parts of individual neurones (e.g. soma *vs.* proximal dendrite) may have contributed to this variability. In Fig. 5*D*, we give an example comparison of the time-dependent change in charge transfer for the inspiratory drive current of a representative microcystin-dialysed inspiratory neurone to that of a representative control inspiratory neurone, i.e. recorded with exactly the same pipette solution except for microcystin. The decline in the relative charge transfer under control conditions may be due to the effects of intracellular dialysis by the control pipette solution.

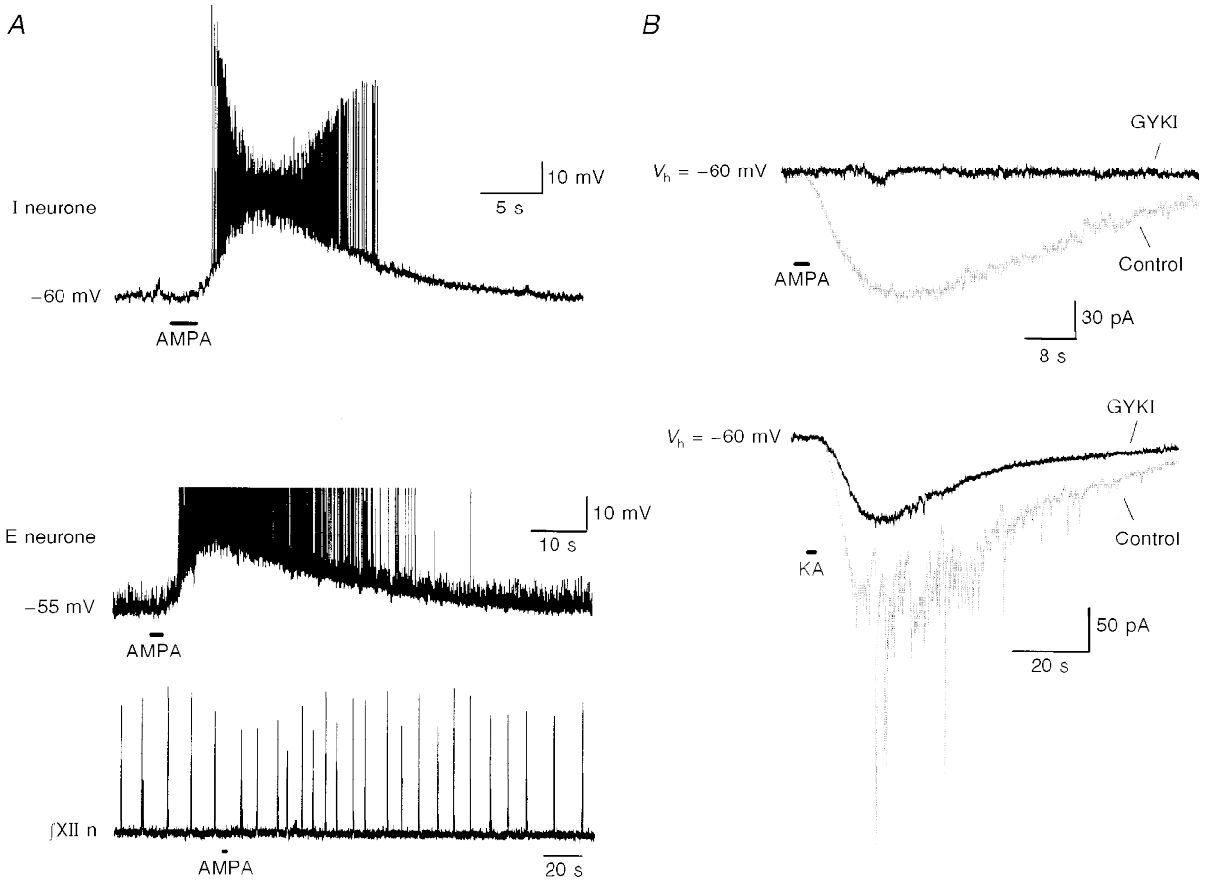

Figure 3. GYKI completely blocked local AMPA-induced current, but not kainate-induced current, in preBötC respiratory neurones

A, local application of AMPA (100 μM, 2 s) at the preBötC depolarized an inspiratory neurone (top; $V_m = -60$ mV) and an expiratory neurone (middle; $V_m = -55$ mV, action potential truncated). The respiratory frequency in XII nerve discharge (bottom) recorded simultaneously with the expiratory neurone also increased. *B*, top, in the presence of TTX (0·5 μM), bath application of GYKI (50 μM) completely blocked AMPA-induced (100 μM, 2 s) current (GYKI, 12 min after GYKI application; holding potential, $V_h = -60$ mV). Bottom, in the presence of TTX (0·5 μM), GYKI (50 μM) partially reduced kainate-induced (KA; 1·0 mM, 2 s) current (GYKI, 14 min after GYKI application; $V_h = -60$ mV). The fast components in control kainate-induced current appeared in three out of the four neurones.

Slight changes in steady-state membrane potential/current were observed in two out of the ten microcystin-dialysed inspiratory neurones. One neurone hyperpolarized shortly (3 min) after whole-cell break-in, but the steady-state membrane potential stabilized 1–2 min later; the other inspiratory neurone slightly depolarized during the enhancement of inspiratory drive.

To establish the effect of phosphorylation on exogenous AMPA-induced currents, TTX (1 μM) was bath applied immediately upon obtaining successful patch recording of an inspiratory neurone ($V_h = -60$ mV; $n = 7$). After TTX had completely abolished synaptic activity, AMPA (100 μM) was locally applied to the preBötC. The ratio of maximal enhancement of AMPA-induced charge transfer (with respect to the state at the beginning of each recording) was averaged amongst inspiratory neurones dialysed with microcystin ($n = 4$; 187 $\pm$ 27%, mean $\pm$ S.E.M.), and amongst the control inspiratory neurones ($n = 3$; 68 $\pm$ 12%) (Fig. 6*C*). Microcystin enhanced the exogenous AMPA-induced current ($P < 0{\cdot}05$, Student's t test). Figure 6*A* shows the current induced by exogenous AMPA (1 s) at various times after membrane rupture in a typical microcystin-dialysed inspiratory neurone; the enhanced AMPA-induced current was subsequently blocked by bath application of GYKI. The time-dependent change in

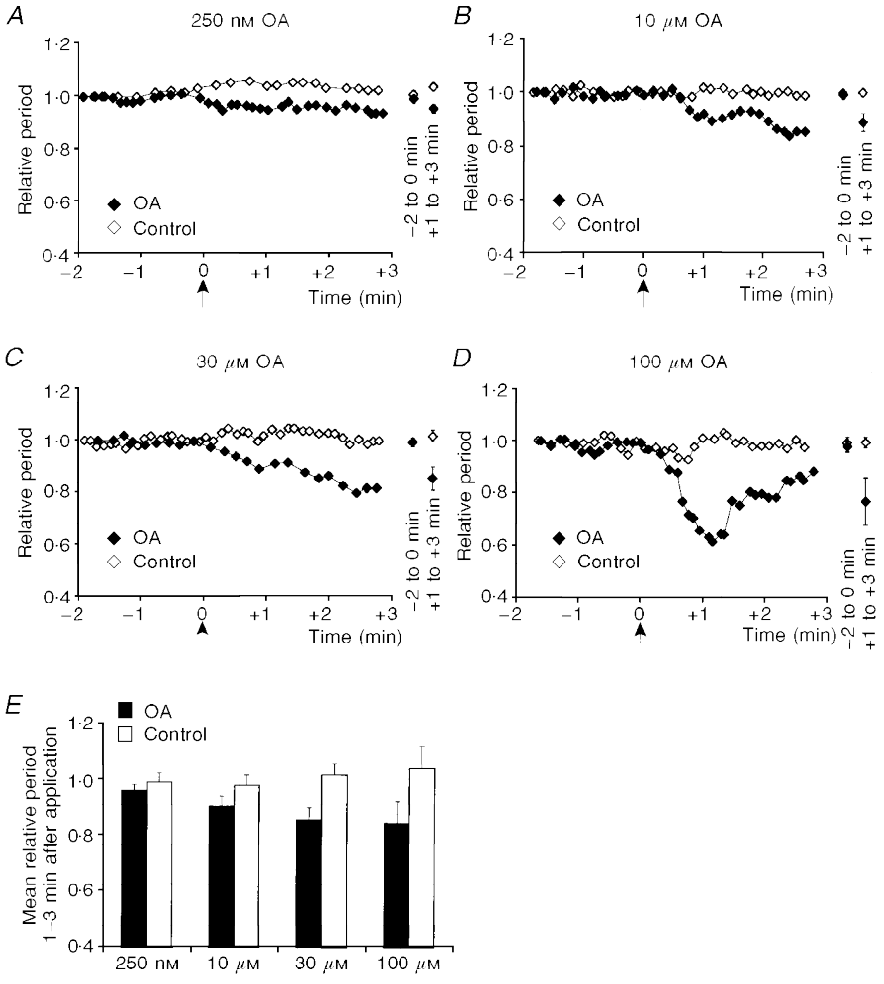

Figure 4. Local application of okadaic acid (OA) within the preBötC increased the respiratory rhythm frequency of the XII nerve

A–D, normalized period of XII nerve recorded with OA (250 nM, 10 μM, 30 μM and 100 μM) injected within the preBötC compared with corresponding control. Arrow in each panel indicates the application of 20 nl OA or control solution. The mean and standard deviation for the XII nerve periods at 2 min before, and 1–3 min after, the application is shown on the right. *E*, the mean XII nerve period at 1–3 min after each application was normalized according to the mean period during 2 min before the application. We then obtained the average and standard deviation of the normalized means for each concentration of OA or the corresponding control solution (250 nM, $n = 5$; control, $n = 4$: 10 μM, $n = 6$; control, $n = 4$: 30 μM, $n = 4$; control, $n = 3$: 100 μM, $n = 4$; control, $n = 4$). OA decreased the respiratory rhythm period of the XII nerve in a concentration-dependent manner ($P < 0{\cdot}05$, non-linear regression).

AMPA-induced charge transfer/peak current for this inspiratory neurone was compared with that of a representative control inspiratory neurone (Fig. 6*B*). Similar to the endogenous response, the effect of microcystin was transient, and the time to maximum increase in AMPA-induced current varied amongst the inspiratory neurones.

Among the microcystin-dialysed inspiratory neurones studied in the presence of TTX, one exhibited a small inward current during the period when AMPA-induced current increased; another inspiratory neurone transiently exhibited an inward current, which stabilized at the original level (−70 pA). Enhancement of AMPA-induced current in this neurone was observed after steady-state membrane current was stabilized.

In order to compare directly the time course of change in charge transfers of endogenous inspiratory drive and exogenous AMPA-induced current, both currents were monitored simultaneously in several microcystin-dialysed

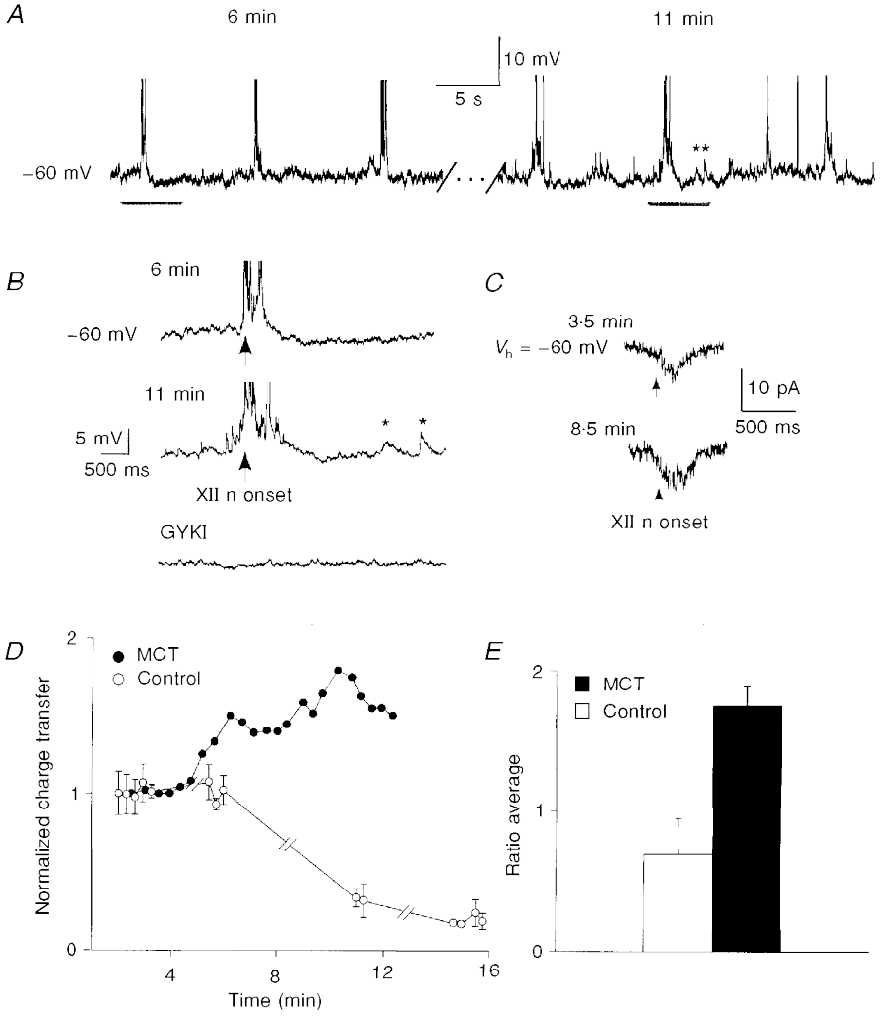

Figure 5. Intracellular dialysis of microcystin enhanced endogenous inspiratory drives in the preBötC inspiratory neurones

A, activity of a microcystin-dialysed (50 μM) inspiratory neurone ($I_h = -64$ pA; $V_m = -60$ mV) at 6 min (left) and 11 min (right) after whole-cell break-in. (Action potentials truncated.) *B*, expanded inspiratory drive potential from each period as indicated by bars under the traces in *A*. Top, 6 min. Middle, 11 min. Asterisks illustrate enhanced sEPSPs. Bottom, GYKI (50 μM) completely blocked enhanced inspiratory drive and sEPSPs. Arrows indicate onset of inspiratory XII nerve burst, which was also blocked by GYKI (not shown). *C*, average of three consecutive inspiratory drive currents at 3·5 min (top) and at 8·5 min (bottom) after whole-cell break-in of another microcystin-dialysed (50 μM) inspiratory neurone ($V_h = -60$ mV). Arrows indicate onset of inspiratory XII nerve burst. *D*, charge transfer in a microcystin-dialysed (MCT) inspiratory neurone (●) and a control inspiratory neurone (○). *E*, average normalized ratio of maximal enhancement in inspiratory drive charge transfer for inspiratory neurones with microcystin ($n = 5$; ■), and control inspiratory neurones ($n = 3$; □; $P < 0{\cdot}05$, Student's unpaired t test). Since no apparent enhancement was observed in control inspiratory neurones, inspiratory drive currents at 20 min after break-in were used for the comparable values.

inspiratory neurones (Fig. 6*D*; $n = 4$) without TTX. Phosphatase inhibition by microcystin caused nearly concurrent enhancement in these currents (Fig. 6*D*).

In inspiratory neurones dialysed with microcystin, input conductance increased ($n = 7$) along with the enhanced AMPA-induced currents; it then decreased when the AMPA-induced charge transfer passed its maximum. Since no significant simultaneous change in steady-state membrane current/potential was observed, this conductance change might reflect enhancement of opening states or numbers of AMPA receptors (or other receptors/channels) affecting steady-state excitability (see Discussion).

Effect of phosphatase inhibition on expiratory neurones

Intracellular microcystin (50 μM) enhanced the amplitude of sEPSPs/sEPSCs in expiratory neurones ($n = 9$). Figure 7*A* compares the sEPSCs of a microcystin-dialysed expiratory neurone at 6 and 11·5 min after whole-cell break-in. In the presence of TTX, intracellular microcystin also increased the local AMPA-induced current in expiratory neurones ($n = 7$; Fig. 7*B*). Similar to inspiratory neurones, the enhancement in sEPSCs and AMPA-induced current (without TTX) in microcystin-dialysed expiratory neurones occurred nearly concurrently ($n = 3$; Fig. 7*C*). The above observations did not occur in the control expiratory neurones ($n = 5$; data not shown).

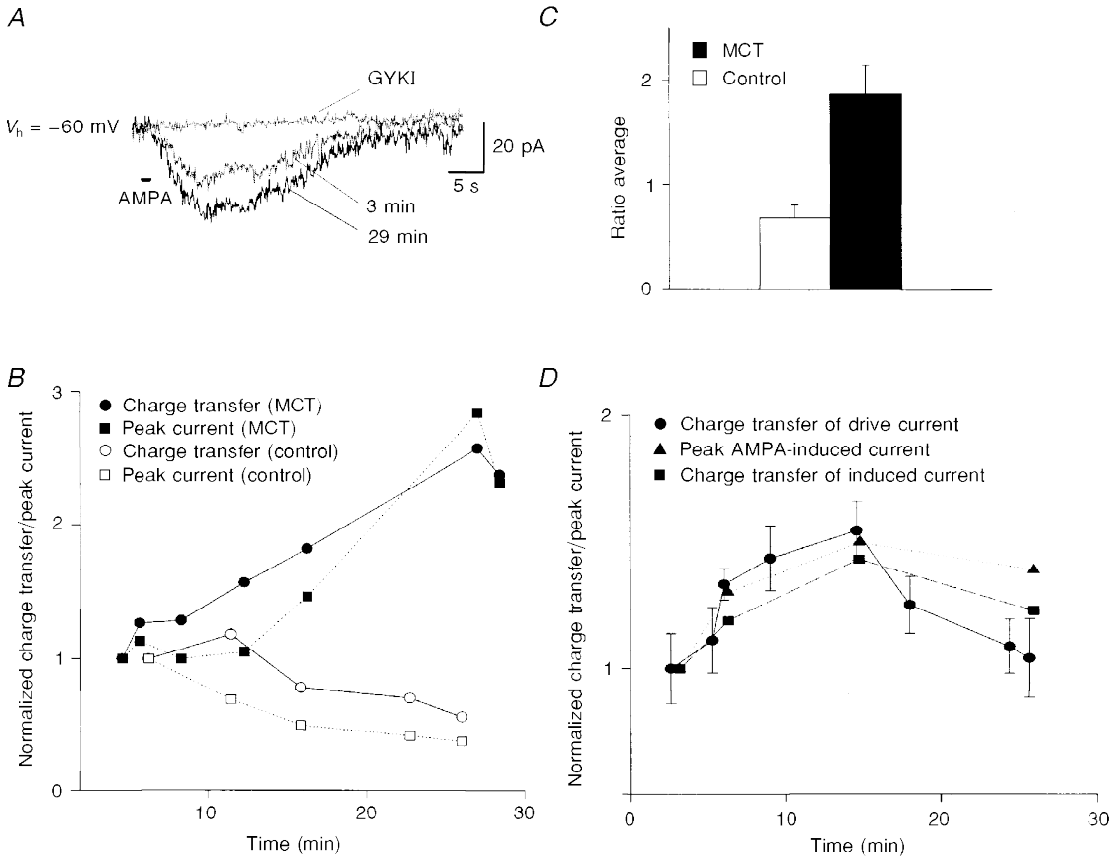

Figure 6. Intracellular dialysis of microcystin enhanced exogenous AMPA-induced currents of preBötC inspiratory neurones in the presence of TTX

A, currents induced by exogenous AMPA (100 μM, 1 s) at 3 min and at 29 min after break-in of a microcystin-dialysed (50 μM) inspiratory neurone ($V_h = -60$ mV; 1 μM TTX). Bath application of GYKI (66·5 μM) completely blocked the increased AMPA-induced current. *B*, time-dependent change in AMPA-induced peak current (■) and charge transfer (●) in the inspiratory neurone shown in *A*, and a control inspiratory neurone ($V_h = -60$ mV; ○, charge transfer; □, peak current). *C*, average normalized ratio of maximal enhancement in AMPA-induced charge transfer for inspiratory neurones with microcystin (MCT, ■; $n = 4$) and control inspiratory neurones (□; $n = 3$; $P < 0{\cdot}05$, Student's unpaired t test). Since no apparent enhancement was observed in control inspiratory neurones, AMPA-induced currents at 20 min after break-in were used to compare with the states at the beginning of the recordings. *D*, without TTX present, microcystin (50 μM) concurrently enhanced inspiratory drive currents and AMPA-induced (100 μM, 2 s) currents in the inspiratory neurone ($V_h = -60$ mV; ●, average normalized charge transfer of three consecutive inspiratory drive currents; ■ and ▲, normalized charge transfer and peak current of AMPA-induced currents, respectively).

DISCUSSION

Activated AMPA receptors and their regulation play an important role in neonatal respiratory rhythm generation and modulation *in vitro*. Blocking AMPA receptors with GYKI in the preBötC, the hypothesized site of respiratory rhythm generation (Smith *et al.* 1991), completely abolished respiratory motor discharge and rhythmic drives in respiratory neurones, while local application of AMPA to the preBötC increased respiratory frequency and depolarized respiratory neurones. GYKI also completely blocked the inward current induced by AMPA but not by kainate in preBötC respiratory neurones. Moreover, phosphatase inhibition within the preBötC modulated the rhythm-generating network by increasing the frequency of respiratory-related discharge. Intracellular inhibition of the same phosphatases enhanced inspiratory synaptic drive and exogenous AMPA-induced current in preBötC inspiratory neurones; both currents were completely blocked by GYKI.

AMPA receptors primarily mediate inspiratory drives in inspiratory neurones

Unlike 6-cyano-7-dinitroquinoxaline-2,3-dione (CNQX) or 6,7-dinitroquinoxaline-2,3-dione (DNQX), the blocking effect of GYKI is not influenced by phasic changes in glutamate concentration, nor is its effect reduced by increasing agonist, e.g. AMPA, concentrations (Donevan & Rogawski, 1993; Zorumski *et al.* 1993; Paternain *et al.* 1995; Wilding & Huettner, 1995). The non-competitive nature of GYKI has made it useful (Paternain *et al.* 1995) for differentiating currents mediated by AMPA or kainate receptors. In addition, because GYKI completely blocks AMPA receptor-mediated currents, including the current induced by kainate, but minimally affects kainate-induced current through kainate receptors, it can uncover the functional role played by kainate receptors (Paternain *et al.* 1995).

We compared endogenous respiratory drive in preBötC respiratory neurones and the current induced by exogenous

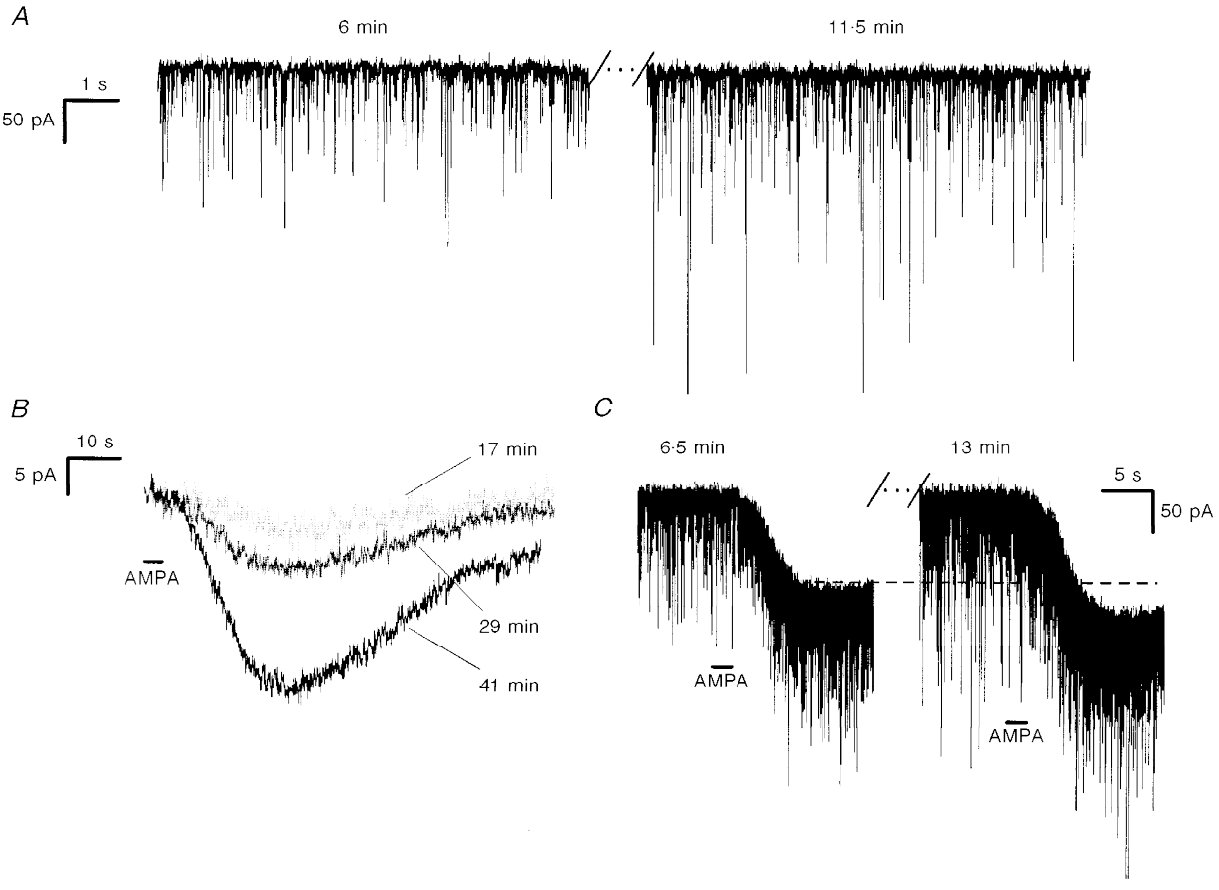

Figure 7. Intracellular dialysis of microcystin concurrently enhanced endogenous sEPSCs and exogenous AMPA-induced currents in preBötC expiratory neurones

A, sEPSCs during expiratory period of a microcystin-dialysed (50 μM) expiratory neurone ($V_h = -60$ mV) at 6 min (left) and 11·5 min (right) after whole-cell break-in. *B*, currents induced by exogenous AMPA (100 μM, 3 s) at 17, 29 and 41 min after whole-cell break-in of a microcystin-dialysed (50 μM) expiratory neurone ($V_h = -60$ mV; 1 μM TTX). *C*, concurrent enhancement of the endogenous sEPSCs and the exogenous AMPA-induced (100 μM, 2 s) current in a microcystin-dialysed (50 μM) expiratory neurone 6·5 min (left) and 13 min (right) after whole cell break-in ($V_h = -60$ mV).

AMPA or kainate, before and after GYKI application. GYKI completely blocked the endogenous respiratory drive, sEPSPs and exogenous AMPA-induced current, but not the exogenous kainate-induced current in preBötC respiratory neurones. Therefore, kainate receptors, while present in the respiratory neurones, are unlikely to be the principal mediator of excitatory synaptic transmission in respiratory rhythmogenesis, since both the respiratory-modulated synaptic currents and rhythmic XII nerve motor discharge were completely blocked by bath or local application of GYKI. Thus, in the neural network that generates respiratory rhythm, AMPA, but not kainate, receptors appear to mediate primarily inspiratory drive and sEPSPs, and are essential for the rhythm and pattern generation. It is not surprising that glutamate, the ubiquitous fast excitatory neurotransmitter in mammalian brain, mediates respiratory drive (Greer *et al.* 1991), but why should AMPA receptors be the principal transducer? For reliable neurotransmission under a wide range of ventilatory demands and neuronal excitability essential for breathing, AMPA receptors are suitable. Moreover, we hypothesize that the possibility that AMPA receptors in these neurones can be modulated by other inputs affecting their phosphorylation state provides them with properties appropriate for their vital homeostatic function. Further illumination of the specific properties of AMPA receptors in respiratory neurones and their particular roles in the central networks controlling breathing will be necessary to test this hypothesis.

Phosphatase inhibition regulates AMPA receptor-mediated respiratory excitability

A member of the glutamate receptor family, AMPA receptor function is regulated by phosphorylation (Greengard *et al.* 1991; Figurov, Boddeke & Muller, 1993; McGlade-McCulloh *et al.* 1993; Kolaj, Cerne, Cheng, Brickey & Randić, 1994; Wang *et al.* 1994*a*; Wyllie & Nicoll, 1994; Yakel *et al.* 1995; Roche *et al.* 1996; Barria *et al.* 1997). Neurones in brain regions other than the preBötC have AMPA receptor subunits that are phosphorylated directly (McGlade-McCulloh *et al.* 1993; Blackstone *et al.* 1994; Tan *et al.* 1994; Nakazawa *et al.* 1995; Yakel *et al.* 1995; Roche *et al.* 1996). Even though the specific phosphorylation sites on AMPA receptor subunits remain equivocal, a consensus is that phosphorylation can occur at multiple sites and involve different protein kinases and phosphatases. Protein kinases that phosphorylate AMPA receptor subunits include: Ca^{2+}–calmodulin-dependent protein kinase II (Ca^{2+}–CaMKII), protein kinase A (PKA), and protein kinase C (PKC); active phosphatases include phosphatase 1, 2A and 2B (calcineurin) (Greengard *et al.* 1991; Figurov *et al.* 1993; McGlade-McCulloh *et al.* 1993; Blackstone *et al.* 1994; Kolaj *et al.* 1994; Tan *et al.* 1994; Wang *et al.* 1994*a*; Wyllie & Nicoll, 1994; Nakazawa *et al.* 1995; Yakel *et al.* 1995; Roche *et al.* 1996). Different AMPA receptor subunits may combine to form the receptor channel (Jonas & Burnashev, 1995), each of which might be affected differently by phosphorylation.

The burst frequency of the XII nerve respiratory discharge increased in a concentration-dependent manner when okadaic acid was applied to the preBötC. This network effect reflects the altered states of, and thus interactions among, its constituent neurones, including inspiratory and expiratory neurones. Enhanced phosphorylation may also have induced network reconfiguration.

In inspiratory and expiratory neurones of the preBötC, intracellular microcystin increased excitability by enhancing sEPSPs and the current induced by exogenous AMPA. Of most interest with respect to generation of respiratory pattern is that intracellular microcystin enhanced the endogenous inspiratory drive currents in inspiratory neurones, which were presumably mediated by AMPA receptors (see above). We propose that these effects were due to alteration of the phosphorylation state of one or more proteins that specifically affect AMPA receptor function in preBötC respiratory neurones; the target proteins could be subunits of the AMPA receptor itself. We did not pursue the mechanism underlying enhanced respiratory drive or the AMPA-induced currents due to phosphatase inhibition. Possible mechanisms include: prolonged channel opening time (Greengard *et al.* 1991; Lieberman & Mody, 1994); increased probability of opening (Greengard *et al.* 1991; Wang, Orser, Brautigan & MacDonald, 1994*b*); or additional recruitment of functional postsynaptic receptors (Isaac, Nicoll & Malenka, 1995; Liao, Hessler & Malinow, 1995; Durand, Kovalchuk & Konnerth, 1996).

The phosphorylation state of other receptors and/or voltage-gated channels might also be affected by okadaic acid or microcystin. However, while there was significant enhancement of endogenous inspiratory drives or exogenous AMPA-induced currents in microcystin-dialysed inspiratory neurones, most neurones exhibited an increase in conductance without an associated change in steady-state membrane current. The increase in conductance may be due to an enhanced opening state of tonically activated AMPA receptors, or other receptors/channels.

We used an elevated K^+ concentration in the bath solution to maintain a robust respiratory-related rhythm in the slice. We recognize that this situation might have caused an increase in inward Ca^{2+} currents due to the depolarization, and thus affected the activities of Ca^{2+}–CaMKII, PKA or PKC. However, since both control and test observations were made under similar conditions, our results indicate that phosphatase inhibition can still significantly enhance respiratory neuronal excitability.

Since the slice preparation we used for these experiments generates an integrative nervous system behaviour, i.e. respiratory-related motor outflow, interpretation of results in the context of function is possible. The functional relevance of the present results is considerable, suggesting that respiratory-modulated excitatory postsynaptic currents, mediated primarily by AMPA receptors, can be altered by

phosphorylation and dephosphorylation of these receptors or associated proteins.

We hypothesize that AMPA receptor function is modulated in respiratory neurones to regulate the net inward inspiratory or expiratory current that is produced for a given amount of presynaptic inspiratory or expiratory activity, ultimately to affect the strength and timing of respiratory muscle contractions that produce breathing movements appropriate for blood gas homeostasis. This modulation could play a role in adjusting ventilation to changes in respiratory demand, such as during exercise, hypoxia (due to disease or altitude), hypercapnia, hyperthermia and sleep. We further hypothesize that this modulation is achieved, at least in part, by phosphorylation and dephosphorylation of AMPA receptors.

In conclusion, we have shown that AMPA receptor activation is crucial for neonatal respiratory rhythm generation. We have also provided evidence of the modulation of synaptic efficacy by phosphatase inhibition in the neural network generating breathing rhythm. Control of the phosphorylation state of AMPA receptor subunits or associated proteins may be an essential component of the mechanisms regulating respiration, and a target site of various neuromodulators, such as serotonin, noradrenaline and various peptides that affect breathing.

Barria, A., Muller, D., Derkach, V., Griffith, L. C. & Soderling, T. R. (1997). Regulatory phosphorylation of AMPA-type glutamate receptors by CaM-KII during long-term potentiation. *Science* **276**, 2042–2045.

Blackstone, C., Murphy, T. H., Moss, S. J., Baraban, J. M. & Huganir, R. L. (1994). Cyclic AMP and synaptic activity-dependent phosphorylation of AMPA-preferring glutamate receptors. *Journal of Neuroscience* **14**, 7585–7593.

Connelly, C. A., Otto-Smith, M. R. & Feldman, J. L. (1992). Blockade of NMDA receptor-channels by MK-801 alters breathing in adult rats. *Brain Research* **596**, 99–110.

Diamond, J. S. & Jahr, C. E. (1995). Asynchronous release of synaptic vesicles determines the time course of the AMPA receptor-mediated EPSC. *Neuron* **15**, 1097–1107.

Donevan, S. D. & Rogawski, M. A. (1993). GYKI 52466, a 2,3-benzodiazepine, is a highly selective, non-competitive antagonist of AMPA/kainate receptor responses. *Neuron* **10**, 51–59.

Durand, G. M., Kovalchuk, Y. & Konnerth, A. (1996). Long-term potentiation and functional synapse induction in developing hippocampus. *Nature* **381**, 71–75.

Figurov, A., Boddeke, H. & Muller, D. (1993). Enhancement of AMPA-mediated synaptic transmission by the protein phosphatase inhibitor calyculin A in rat hippocampal slices. *European Journal of Neuroscience* **5**, 1035–1041.

Funk, G. D., Johnson, S. M., Smith, J. C., Dong, X.-W., Lai, J. & Feldman, J. L. (1997). Functional respiratory rhythm generating networks in neonatal mice lacking NMDAR1 gene. *Journal of Neurophysiology* **78**, 1414–1420.

Funk, G. D., Smith, J. C. & Feldman, J. L. (1993). Generation and transmission of respiratory oscillations in medullary slices: role of excitatory amino acids. *Journal of Neurophysiology* **70**, 1497–1515.

Funk, G. D., Smith, J. C. & Feldman, J. L. (1995). Modulation of neural network activity *in vitro* by cyclothiazide, a drug that blocks desensitization of AMPA receptors. *Journal of Neuroscience* **15**, 4046–4056.

Greengard, P., Jen, J., Nairn, A. C. & Stevens, C. F. (1991). Enhancement of the glutamate response by cAMP-dependent protein kinase in hippocampal neurons. *Science* **253**, 1135–1138.

Greer, J. J., Smith, J. C. & Feldman, J. L. (1991). Role of excitatory amino acids in the generation and transmission of respiratory drive in neonatal rat. *Journal of Physiology* **437**, 727–749.

Isaac, J. T., Nicoll, R. A. & Malenka, R. C. (1995). Evidence for silent synapses: implications for the expression of LTP. *Neuron* **15**, 427–434.

Ito, I., Tanabe, S., Kohda, A. & Sugiyama, H. (1990). Allosteric potentiation of quisqualate receptors by a nootropic drug aniracetam. *Journal of Physiology* **424**, 533–543.

Jonas, P. & Burnashev, N. (1995). Molecular mechanisms controlling calcium entry through AMPA-type glutamate receptor channels. *Neuron* **15**, 987–990.

Kolaj, M., Cerne, R., Cheng, G., Brickey, D. A. & Randić, M. (1994). Alpha subunit of calcium/calmodulin-dependent protein kinase enhances excitatory amino acid and synaptic responses of rat spinal dorsal horn neurons. *Journal of Neurophysiology* **72**, 2525–2531.

Lerma, J., Paternain, A. V., Naranjo, J. R. & Mellström, B. (1993). Functional kainate-selective glutamate receptors in cultured hippocampal neurons. *Proceedings of the National Academy of Sciences of the USA* **90**, 11688–11692.

Liao, D., Hessler, N. A. & Malinow, R. (1995). Activation of postsynaptically silent synapses during pairing-induced LTP in CA1 region of hippocampal slice. *Nature* **375**, 400–404.

Lieberman, D. N. & Mody, I. (1994). Regulation of NMDA channel function by endogenous Ca^{2+}-dependent phosphatase. *Nature* **369**, 235–239.

McGlade-McCulloh, E., Yamamoto, H., Tan, S.-E., Brickey, D. A. & Soderling, T. R. (1993). Phosphorylation and regulation of glutamate receptors by calcium/calmodulin-dependent protein kinase II. *Nature* **362**, 640–642.

Nakazawa, K., Mikawa, S., Hashikawa, T. & Ito, M. (1995). Transient and persistent phosphorylation of AMPA-type glutamate receptor subunits in cerebellar purkinje cells. *Neuron* **15**, 697–709.

Paternain, A. V., Morales, M. & Lerma, J. (1995). Selective antagonism of AMPA receptors unmasks kainate receptor-mediated responses in hippocampal neurons. *Neuron* **14**, 185–189.

Patneau, D. K., Wright, P. W., Winters, C., Mayer, M. L. & Gallo, V. (1994). Glial cells of the oligodendrocyte lineage express both kainate- and AMPA-preferring subtypes of glutamate receptor. *Neuron* **12**, 357–371.

Pierrefiche, O., Foutz, A. S., Champagnat, J. & Denavit-Saubié, M. (1994). NMDA and non-NMDA receptors may play distinct roles in timing mechanisms and transmission in the feline respiratory network. *Journal of Physiology* **474**, 509–523.

Roche, K. W., O'Brien, R. J., Mammen, A. L., Bernhardt, J. & Huganir, R. L. (1996). Characterization of multiple phosphorylation sites on the AMPA receptor GluR1 subunit. *Neuron* **16**, 1179–1188.

Smith, J. C., Ellenberger, H. H., Ballanyi, K., Richter, D. W. & Feldman, J. L. (1991). Pre-Bötzinger complex: a brainstem region that may generate respiratory rhythm in mammals. *Science* **254**, 726–729.

Tan, S.-E., Wenthold, R. J. & Soderling, T. R. (1994). Phosphorylation of AMPA-type glutamate receptors by calcium/calmodulin-dependent protein kinase II and protein kinase C in cultured hippocampal neurons. *Journal of Neuroscience* **14**, 1123–1129.

Trussell, L. O., Zhang, S. & Raman, I. M. (1993). Desensitization of AMPA receptors upon multiquantal neurotransmitter release. *Neuron* **10**, 1185–1196.

Wang, L.-Y., Dudek, E. M., Browning, M. D. & MacDonald, J. F. (1994*a*). Modulation of AMPA/kainate receptors in cultured murine hippocampal neurones by protein kinase C. *Journal of Physiology* **475**, 431–437.

Wang, L.-Y., Orser, B. A., Brautigan, D. L. & MacDonald, J. F. (1994*b*). Regulation of NMDA receptors in cultured hippocampal neurons by protein phosphatases 1 and 2A. *Nature* **369**, 230–232.

Wilding, T. J. & Huettner, J. E. (1995). Differential antagonism of α-amino-3-hydroxy-5-methyl-4-isoxazolepropionic acid-preferring and kainate-preferring receptors by 2,3-benzodiazepines. *Molecular Pharmacology* **47**, 582–587.

Wyllie, D. J. & Nicoll, R. A. (1994). A role for protein kinases and phosphatases in the Ca^{2+}-induced enhancement of hippocampal AMPA receptor-mediated synaptic responses. *Neuron* **13**, 635–643.

Yakel, J. L., Vissavajjhala, P., Derkach, V. A., Brickey, D. A. & Soderling, T. R. (1995). Identification of a Ca^{2+}/calmodulin-dependent protein kinase II regulatory phosphorylation site in non-*N*-methyl-D-aspartate glutamate receptors. *Proceedings of the National Academy of Sciences of the USA* **92**, 1376–1380.

Zorumski, C. F., Yamada, K. A., Price, M. T. & Olney, J. W. (1993). A benzodiazepine recognition site associated with the non-NMDA glutamate receptor. *Neuron* **10**, 61–67.

Acknowledgements

This work was supported by a grant (HL40959) from the National Institutes of Health. The authors particularly thank Dr Xuesi M. Shao for his support, technical help, and constructive discussions throughout the project, and our colleagues at the Systems Neurobiology Laboratory for critical comments on the manuscript. Q.G. thanks Dr Steven M. Johnson for teaching the slice preparation technique.

Corresponding author

J. L. Feldman: Department of Neurobiology, Box 951763, University of California, Los Angeles, CA 90095-1763, USA.

Email: feldman@ucla.edu